

Effect of Induced Hepatic Ischemia–Reperfusion on the Adrenal Cortex of Adult Male Albino Rats and the Possible Protective Role of L-Arginine: Biochemical, Histological and Immunohistochemical Study

Amira Fahmy Ali and Nadia Said Badawy khair

Department of Histology, Faculty of Medicine; Menoufia University, Egypt

ABSTRACT

Introduction: Hepatic ischemia reperfusion injury (IRI) takes place through liver transplantation. Hepatic IRI might seriously affect liver function and is reported to be accountable for 15 % of organ failure and could result in multi-organ dysfunction syndrome (MODS) that lead to high rates of morbidity and mortality. L-arginine (L-Arg) could reduce hepatic IRI via different mechanisms

Objective: To estimate the effect of hepatic ischemic reperfusion (I/R) and the possible protective effect of L-Arg. on the adrenal cortex.

Materials and Methods: Thirty two albino rats were utilized in the current work. The animals split to Sham-Operation, L-Arg, ischemic reperfusion, I/R group and I/R and L-Arg group. Then, at the assigned time, blood samples were assembled for biochemical study. Histological and immunohistochemical studies were performed on the adrenal tissue.

Results: The adrenal cortex of I/R group exhibited architecture loss of the three zones. Zona glomerulosa cells showed small pyknotic nuclei and vacuolated cytoplasm. Zona fasciculata cells appeared ballooned with small pyknotic nuclei. Also, karyolitic nuclei were seen. zona reticularis cells showed pyknotic nuclei and vacuolated cytoplasm and separated by congested blood sinusoids. Hyaline material depositions were seen. Biochemical study revealed a marked increase in serum levels of liver enzymes, excess in the MDA level and a marked reduction in the CAT level compared to control group. These changes were ameliorated by L-Arg.

Conclusion: Hepatic I/R has been proved to induce histological changes of the adrenal cortex which could be ameliorated by administration of L-Arg. Therefore, For inhibiting or reducing hepatic IRI through liver surgery, an effective method is urgently required.

Received: 04 September 2021, **Accepted:** 14 October 2021

Key Words: Adrenal cortex, ischemic reperfusion, l-arg, TNF- α .

Corresponding Author: Amira Fahmy Ali, MD, Department of Histology, Faculty of Medicine; Menoufia University, Egypt, **Tel.:** +20 10 6891 5402, **E-mail:** amirafahmy356@yahoo.com

ISSN: 1110-0559, Vol. 46, No.1

INTRODUCTION

Ischemia-reperfusion injury (IRI) in the liver is a pathological disease characterised by ischemia-mediated cellular injury followed by a paradoxical worsening upon hepatic reperfusion. Over the last few decades, it has been the subject of significant research, as it is started by hepatocellular injury and takes place through resection surgery and liver transplantation as well as trauma and a hemorrhagic shock^[1]. IRI is not a patho-physiological condition seriously impairs liver function only, even producing irreversible damage but a complex systemic process impacting various organs and tissues, a condition called multi-organ dysfunction syndrome (MODS) and elicit systemic inflammatory response syndrome (SIRS) which have substantial morbidity and fatality rates^[2]. Many mechanisms included in the development of IRI. It comprises several major steps involving, activation of Kupffer cell, cytokine release, polymorphonuclear leukocytes activation, reactive oxygen derivatives

formation, altered mitochondrial permeability, endothelial cell activation, and complement systems^[3,4]. Local and systemic inflammatory reactions are triggered as a result of these events, resulting in organ harm. The lungs, adrenals, gut, myocardium, and kidneys are some of the distant organs that have been affected by hepatic ischemia/reperfusion injury^[5].

The adrenal gland is a substantial endocrine gland which secretes the adrenal hormones^[6]. Its cortical hormones directly affect carbohydrate, protein, and lipids metabolism, therefore, affecting the functional status of all body organs including bones, muscles, heart, liver, kidney, and nervous system^[7]. About 93% of patients underwent liver transplantation, even in steroid free immunosuppressant protocols, exhibited relative adrenal insufficiency, which described as hepato-adrenal syndrome^[8].

L-Arginine (L-Arg) is considered an amino acid and a protein building block, naturally found in poultry, red meat, dairy products and fish. L-Arg appears to

have a crucial function in a variety of biological and physiological processes, according to growing data, in the last two decades^[9]. It is considered as an essential biologically active compound in cellular homeostasis and function. L-arginine is a primary source of nitric oxide (NO), which is produced by nitric oxide synthase enzymes (NOS)^[10]. NO, a signaling molecule that's needed for a variety of bodily processes and functions, including blood flow regulation, mitochondrial function, and cellular communication^[11]. In liver injury models in rats and hepatic ischemia reperfusion injury in pigs, L-Arg exerts a protective role^[12]. In the liver illnesses such as cirrhosis and fatty liver, L-Arginine exhibits immuno-supportive properties^[13]. The studies on the effects of hepatic IRI on the adrenal cortex were few and very limited. Therefore, the aim of the present work was to investigate the impact of hepatic IRI on the structure of the adrenal cortex and the protective effect of L-Arg, using histological, biochemical and immunohistochemical methods.

MATERIAL AND METHODS

Thirty two adult male albino rats, 3 months of age and weighing between 200 and 250 g were utilized in the current work. The animals were housed in metal cages at suitable temperature and were exposed to day light from 10-12 hours. Food and water were freely available to rats. Strict hygiene was followed to keep a healthy medium for rats. All Animals' protocols were authorized and observed via the animal Care Committee of the Research Laboratory of Experimental Animals, Faculty of Medicine, Menoufia University, Egypt.

Drugs and Chemicals

L-Arginine (Cayman chemical company, USA), used in powder form and was fresh prepared by dissolving in distilled water to prepare the desired dose (100mg/kg.bw) according to Sánchez-Fidalgo *et al*^[14].

Thiopental sodium (Pentothal)

Each vial contains 500 mg of Thiopental sodium in 20 ml. It was obtained from Sigma – Tec. Pharmaceutical Industries – Egypt – S.A.E. Each 1 ml of vial was diluted in 4 ml of distilled water for intra-peritoneal injection of the calculated dose.

The rats were split into four equal groups of eight rats each.

1. Group I: (Sham operation, SO)
2. Group II: (L- Arginine (L-Arg) group)
3. Group III: (Ischemia–reperfusion (I/R) group)
4. Group IV: (I/R and L-Arg)

Surgical Technique

All rats were anesthetized by thiopental sodium (25 mg/kg)^[15] through intra-peritoneal injection, repeated as needed. Rats were then laid supine on a warming pad (36–37°C) to keep a constant body temperature. Then

the abdomen was opened (laparotomy) via midline longitudinal incision after shaving and disinfection. The hepatic artery, portal vein, and common bile duct were clamped with microvascular bulldog clamps for 3 hours to achieve ischemia. In order to prevent visceral dehydration, normal saline (37°C) was installed into the abdominal cavity for 10 min and wrapping of the abdomen by plastic covers was done. After the ischemic period, the reperfusion was allowed for another 3 hours by opening the clamps^[16]. Ischemia was verified through the pale appearance of liver and the bluish discoloration upon the reperfusion.

- Sham operation (SO) group: underwent the same standard operation without vascular occlusion.
- L- Arginine (L-Arg) group: rats received L-Arg (100 mg/kg), intraperitoneal^[14] 30 minutes prior to the sham operation's start time.
- Ischemia reperfusion (I/R) group: Following the normal procedure (laparotomy), the portal vein, hepatic artery, and bile ducts were clamped for 3 hours to produce ischemia, then reperused for 3 hours.
- Ischemia–reperfusion and L- Arginine (I/R and L-Arg) group: rats received L-Arg in the same dose as group II, 30 min prior to the ligation, The rest of the surgical procedures were carried out in the same way as in group I/R.

At the assigned time, 2-cc blood sample taken from the abdominal aorta of all groups and rapidly centrifuged. Both adrenal glands were surgically removed for histological and immunohistochemical studies.

I-Biochemical assays

The blood samples were centrifuged for 10 min at room temperature to separate serum for analysis. Sera were stored at –70°C and used for estimation of:

1. Liver enzymes AST and ALT (aspartate transaminase and alanine transaminase) to verify hepatic injury and high density lipoprotein (HDL) (Biodiagnostic, Cairo, Egypt) by enzymatic colorimetric methods^[17].
2. corticosterone and aldosterone levels were determined using a radioimmunoassay kit (Biochemicals, Costa Mesa, CA, USA)^[18].
3. Catalase (CAT)(antioxidant enzyme) by enzymatic colorimetric method (Biodiagnostic)^[19].
4. Malondialdehyde (MDA), as a lipid peroxidation marker^[20]. All biochemical analyses were done in central lab, Faculty of Medicine, Menoufia University.

II-Histological study

The right adrenal gland of each animal was dissected and fixed in 10% formal saline, dehydrated in ascending grades of alcohol, cleared with xylene, and embedded into

paraffin. Then 5 μm sections were cut and stained with hematoxylin and eosin (Hx&E) to observe the histological structure and Mallory's trichrome stain (M.T) to detect the collagen fibers^[21].

III-Electron microscopic study

Small pieces of the left adrenal glands from all animal groups were rapidly fixed in 3% glutaraldehyde solution and processed for examination, utilizing a Jeol- JEM- 100 CXII (Joel, Tokyo, Japan)^[22]. TEM processing and analysis were done at E.M center, Faculty of Science, Alexandria University.

IV-Immunohistochemical study for detection of

A-Activated caspase -3 (apoptotic marker) (purchased as anticaspase -3 rabbit polyclonal antibody, Thermo Scientific, Fermont, California, USA) for detection of apoptotic cortical cells. The reaction was cytoplasmic and nuclear.

B-Tumor necrosis factor - α (index of inflammation). The primary monoclonal antibody utilized was mouse anti-TNF- α (Santa Cruz Biotechnology, California, USA). The reaction was cytoplasmic.

Immunohistochemical staining was carried by avidin-biotin peroxidase method. Sections of adrenal glands were incubated for one hour at 4°C with 1: 100 dilution of the primary antibody. Counterstained with Mayer's hematoxylin. Tonsils were used as positive control in case of caspase-3 while colon was positive control in case of TNF- α ^[23].

V-Morphometric and Statistical analysis

All quantitative data was collected using the "Leica Qwin 500 C" image analyzer automated data processing system Ltd. (Cambridge, England). The thickness of the capsule and adrenal cortex of all groups, were measured in Hx&E stained sections using the distance parameters in the interactive measurement menu, with 10 random non-overlapping fields evaluated using 10 objective lenses. With a total magnification of X400. The area percentage (%) of Caspase-3 and TNF- α immunoreactivity were determined within 10 fields of each rat. The measured variance was estimated using the software version K1.45 of Image J. Significant differences between different groups were reported utilizing the Student t-test and variance test analysis. Statistical significance was defined as a *P* value less than 0.05^[24].

RESULTS

Biochemical results

Liver enzymes and HDL

As shown in (Table 1), group II (L-Arg) exhibited non-significant changes in the liver enzymes and HDL ($P > .05$) in comparison with animals of group I. Group III (I/R group) exhibited a highly significant increase in the serum levels of ALT and AST and a high significant decrease in

HDL ($P < .001$) in comparison with the animals of group I. Moreover, group IV (I/R and L-Arg group) displayed a non-significant changes ($P > .05$) in mean values of these parameters when compared with the control animals. While revealed a highly significant changes ($P < .001$) in comparison with I/R group (Histograms 1,2).

Oxidant/Anti-oxidant markers

Data in (Table 2), showed that group II (L-Arg group) demonstrated non-significant changes in the MDA level and CAT in comparison with animals of group I ($P > .05$). Group III (I/R group) exhibited a highly significant rise in the level of MDA ($P < .05$) and a highly significant decrease ($P < .001$) in the level of CAT in comparison with the animals of control group. Moreover, group IV (I/R and L-Arg group) demonstrated a non-significant changes in the values of MDA and CAT ($P > .05$) when compared with the control animals, while revealed a highly significant increase in the level of antioxidant enzyme ($P < .001$) and a highly significant decrease in MDA level in comparison with I/R group (Histograms 3,4)

Adrenal hormones

As shown in (Table 3), group II (L-Arg group) displayed a non-significant changes in the cortisone and aldosterone levels ($P > 0.05$) in comparison with control animals. Group III (I/R group) displayed a significant decrease in the level of these hormones ($P < .05$) in comparison with the animals of group I. Moreover, group IV (I/R and L-Arg group) displayed a non-significant changes in the mean values of cortisone and aldosterone ($P > .05$) in comparison with the animals of control group, while revealed a significant changes ($P < .05$) in comparison with I/R group (Histogram 5).

Histological results

Haematoxylin & eosin stained adrenal cortex of control rats (groups I&II) were the same and revealed normal histological structure. There were zona glomerulosa (ZG), zona fasciculata (ZF) and finally, zona reticularis (ZR) under the capsule (Figure 1). The cells of ZG were arranged in curved clusters with rounded vesicular nuclei under the capsule. ZF cells were arranged in straight parallel cords of large polyhedral cells separated by blood sinusoids. The cells had central rounded vesicular nuclei and acidophilic vacuolated cytoplasm (Figure 2). ZR cells were arranged in anastomosing cords of closely packed cells with acidophilic cytoplasm and central rounded nuclei (Figure 3).

Group III (I/R group) exhibited histological alterations. Distorted architecture of ZG was observed, the capsule was thickened and corrugated (Figures 4,5). ZG cells appeared with small pyknotic nuclei. ZF cells appeared ballooned with small pyknotic nuclei (Figures 4,5), karyolytic nuclei were seen (Figure 5). ZR cells showed pyknotic nuclei and vacuolated cytoplasm (Figure 6). Hyaline material depositions were seen in ZF and ZR (Figure 6).

Sections of the group IV (I/R and L-Arg group) showed nearly normal appearance of ZG and ZF (Figure 7). ZR cells arranged in anastomosing cords and separated by blood sinusoids (Figure 8).

Mallory's trichrome stained adrenal cortex in control rats (groups I&II) displayed mild amount of regular collagen fibers of the capsule and in the extending trabeculae between the arches of ZG cells (Figure 9). While group III (I/R) was appeared with excess collagen fibers in the capsule and trabeculae (Figure 10). Moreover, group IV (I/R and L-Arg group) revealed moderate amount of collagen fibers (Figure 11).

Ultra-thin sections from the control rats (groups I&II) exhibited a normal ultrastructure of the adrenal cortex zones. ZG cells displayed euchromatic nuclei with perinuclear space. They have vesicular mitochondria, smooth endoplasmic reticulum and intercellular canaliculi were observed between two adjacent cells (Figure 12). ZF cells revealed euchromatic nuclei, numerous spherical mitochondria of variable sizes, smooth endoplasmic reticulum, abundant lipid droplets and numerous free ribosomes (Figure 13). ZR cells contained euchromatic nuclei with perinuclear space. The cytoplasm revealed numerous spherical mitochondria with densely packed vesicular cristae, plenty of smooth endoplasmic reticulum, lipid droplet, and free ribosomes (Figure 14).

An electron microscopic examination of group III (I/R group) revealed alterations of the cells of adrenal cortex zones. ZG cells showed nuclei with irregular nuclear membrane, degenerated mitochondria, dilated smooth endoplasmic reticulum, some lipid droplets. Disrupted intercellular canaliculi between adjacent cells were seen (Figure 15). The cells of ZF contained nucleus with irregular nuclear membrane, degenerated mitochondria and multiple lipid droplets without discernible outline (Figure 16). ZR cell showed nucleus with irregular nuclear membrane and widened perinuclear space. The cytoplasm contained cytoplasmic vacuoles, smooth endoplasmic reticulum, degenerated mitochondria and lipid droplets (Figure 17). While an electron microscopic examination of group IV (I/R and L-Arg group) revealed preservation of the adrenal cortex. Most cells of the three zones appeared more or less similar to the control. Zona glomerulosa cell showed rounded euchromatic nuclei with prominent nucleolus, lipid droplets, numerous mitochondria with vesicular cristae, smooth endoplasmic reticulum, Intercellular canaliculi were seen between two adjacent cells (Figure 18). The cells of Zona fasciculata contained euchromatic nucleus, the other has shrunken nucleus with irregular outline. Lipid droplets, mitochondria, smooth endoplasmic reticulum and free ribosomes were observed. Also, some confluent lipid droplets were seen (Figure 19). Zona reticularis cell revealed slightly irregular euchromatic nucleus, spherical mitochondria of variable sizes with closely packed vesicular cristae, free ribosomes and smooth endoplasmic reticulum (Figure 20).

Immunohistochemical results

Anti-TNF- α immune expression of control groups (groups I&II) revealed negative immunoreactivity in the three zones of adrenal cortex (Figure 21). Group III (I/R group) revealed strong positive cytoplasmic immunoreactivity in the cells of zona glomerulosa, zona fasciculata and zona reticularis (Figure 22). Moreover, group IV (I/R and L-Arg group) exhibited moderate cytoplasmic immunoreactivity in the cells of zona glomerulosa and mild expression in zona fasciculata and zona reticularis (Figure 23).

Anti-caspase-3 immune-marker expression of control groups (groups I&II) displayed negative immunoreactivity in the cells of zona glomerulosa, zona fasciculata and zona reticularis (Figure 24). Group III (I/R group) revealed strong positive nuclear and cytoplasmic immunoreactivity in the cells of zona glomerulosa, zona fasciculata and zona reticularis (Figure 25). While group IV (I/R and L-Arg group) revealed moderate nuclear and cytoplasmic immunoreactivity (Figure 26).

Morphometric and statistical results

Data in (Table 4) demonstrated that group III (I/R group) exhibited a highly significant increase in the thickness of the capsule and a highly significant decrease in the thickness of adrenal cortex ($P < .001$) when compared with the control animals, while group IV (I/R and L-Arg group) revealed a significant change ($P < .05$) in thickness of the capsule and a non significant change ($P > .05$) in the thickness of the adrenal cortex when compared with the control animals. While, revealed a highly significant changes in comparison with I/R group (group III) ($P < .001$) (Histograms 6,7).

Data in (Table 5) showed that group III (I/R group) exhibited a highly significant increase ($P < .001$) in the mean area % of TNF- α and caspase-3 immunoreactions in the adrenal cortex in comparison with group I. However, group IV (I/R and L-Arg group) displayed a highly significant decrease ($P < .001$) in comparison with group III (Histogram 8).

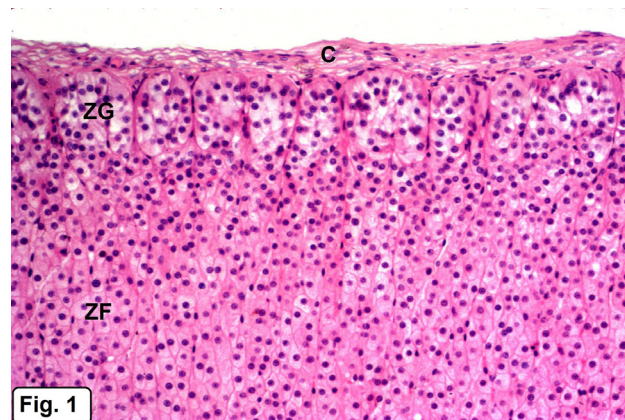


Fig. 1: A section of the adrenal cortex of group I (SO) illustrating capsule (C), zona glomerulosa (ZG) formed of curved clusters of cells and zona fasciculata (ZF) consists of straight parallel cords of cells. Hx&E X100

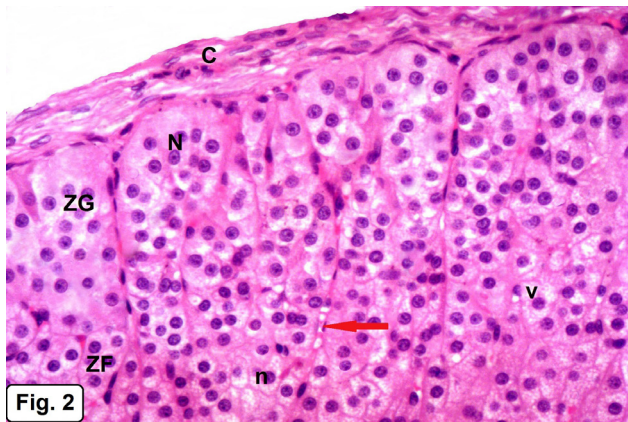


Fig. 2: A section of the adrenal cortex of group I (SO) illustrating capsule (C), zona glomerulosa (ZG) formed of curved clusters of cells with rounded vesicular nuclei (N). The cells of zona fasciculata (ZF) are arranged in straight parallel cords separated by blood sinusoids (red arrow). The cells are polyhedral in shape with central rounded vesicular nuclei (n) and acidophilic vacuolated cytoplasm (V). Hx&E X200

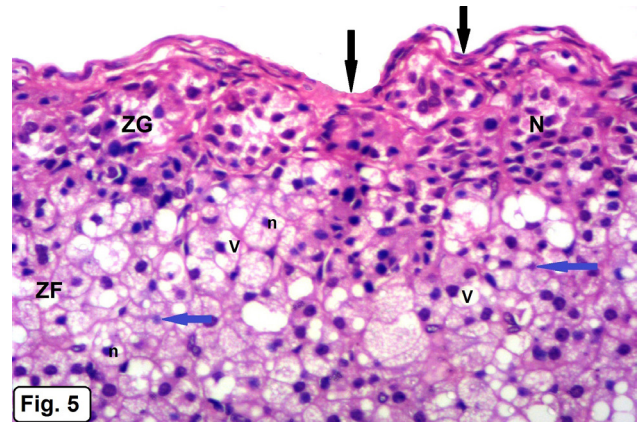


Fig. 5: A section of the adrenal cortex of group III (I/R) illustrating corrugation of the capsule (black arrows) and disorganized zona glomerulosa (ZG) with small pyknotic nuclei (N). The cells of zona fasciculata (ZF) have vacuolated cytoplasm (V) and small pyknotic nuclei (n). Notice, presence of karyolytic nuclei (blue arrows). Hx&E X200

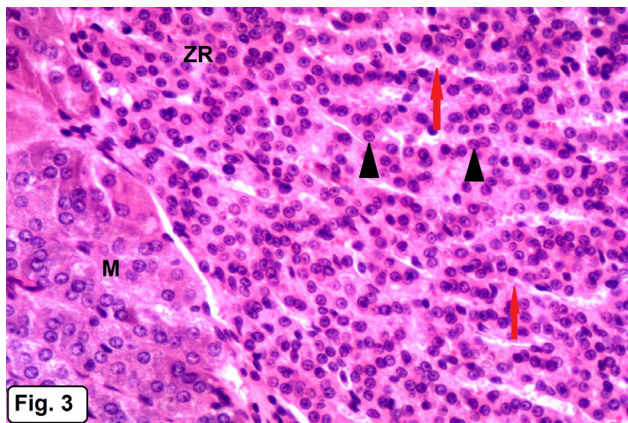


Fig. 3: A section of the adrenal cortex of group I (SO) illustrating zona reticularis (ZR) arranged in anastomosing cords of closely packed cells with central rounded nuclei (arrow heads) and acidophilic cytoplasm. Notice, the cells are separated by blood sinusoids (red arrows). Part of the medulla (M) is also seen. Hx&E X200

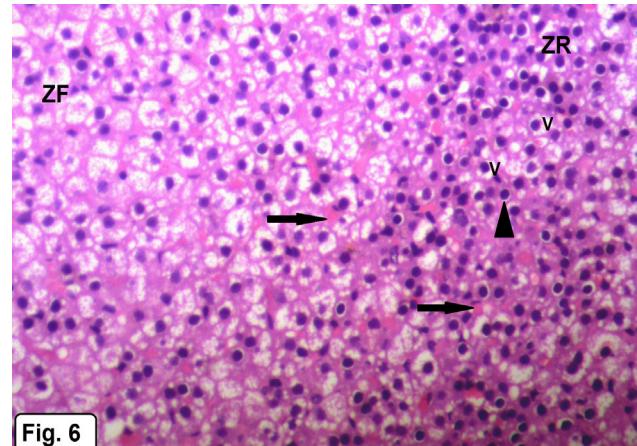


Fig. 6: A section of the adrenal cortex of group III (I/R) illustrating zona reticularis cells with pyknotic nuclei (arrow heads) and vacuolated cytoplasm (V). Hyaline material depositions (black arrows) are seen in zona fasciculata (ZF) and zona reticularis (ZR). Hx&E X200

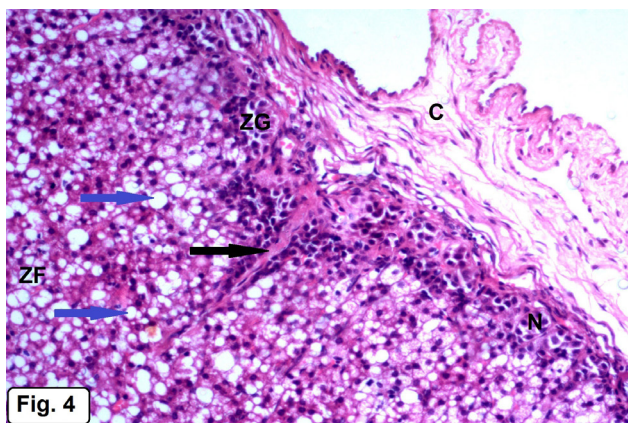


Fig. 4: A section of the adrenal cortex of group III (I/R) illustrating thick capsule (C) and trabeculae (black arrow). Distorted architecture of zona glomerulosa (ZG) with small pyknotic nuclei (N) is seen. The cells of zona fasciculata (ZF) appear ballooned (blue arrows). Hx&E X100

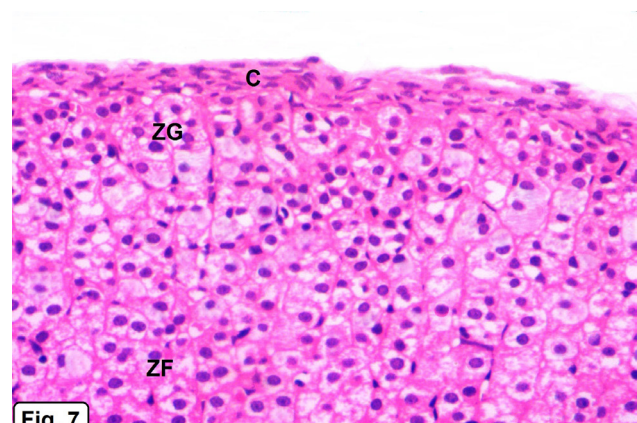


Fig. 7: A section of the adrenal cortex of group IV (I/R and L-Arg) illustrating capsule (C). The cells of zona glomerulosa (ZG) and Zona fasciculata (ZF) appear more or less similar to control. Hx&E X200

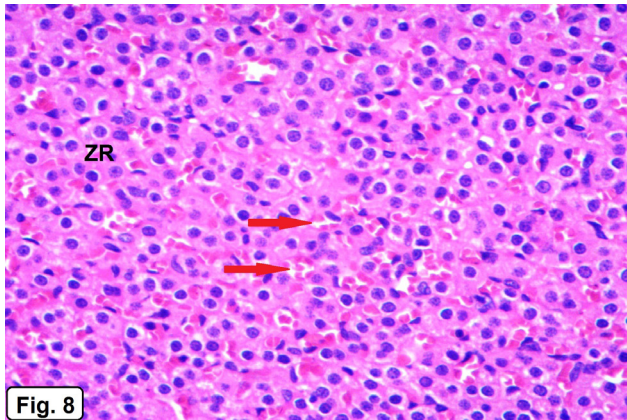


Fig. 8: A section of the adrenal cortex of group IV (I/R and L-Arg) illustrating zona reticularis (ZR) formed of anastomosing cords of closely packed cells separated by blood sinusoids (red arrows). Hx&E X200

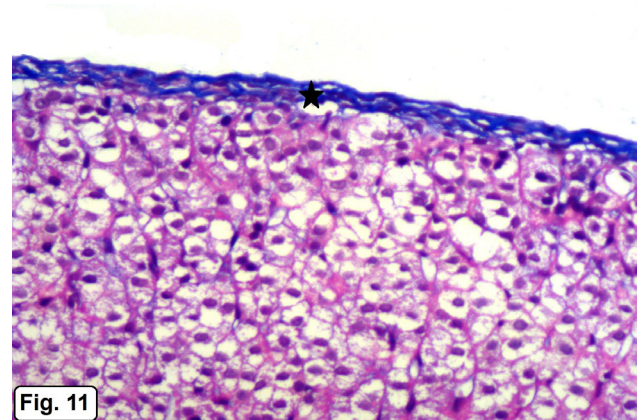


Fig. 11: A section of the adrenal cortex of group IV (I/R and L-Arg) illustrating moderate amount of collagen fibers (star) of the capsule. M.T X200

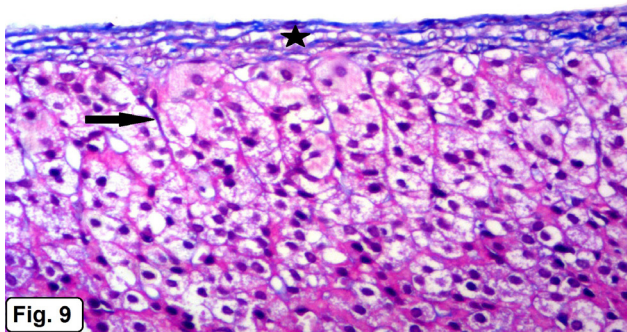


Fig. 9: A section of the adrenal cortex of group I (SO) illustrating mild amount of regular collagen fibers (star) of the capsule and in the extending trabeculae (black arrow) between the arches of zona glomerulosa cells. M.T X200

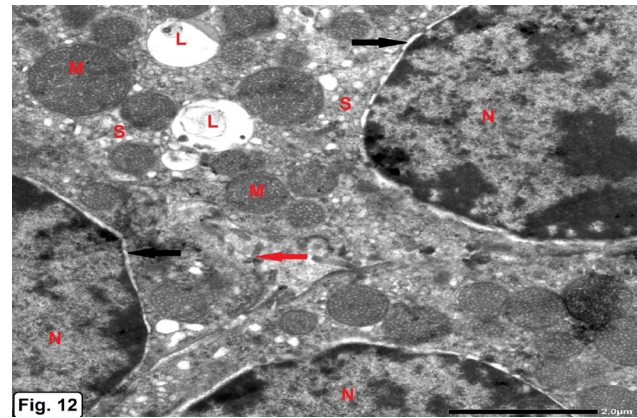


Fig. 12: An electron micrograph of the zona glomerulosa cells of group I (SO) illustrating euchromatic nuclei (N) with perinuclear space (black arrows), vesicular mitochondria (M), smooth endoplasmic reticulum (S) and lipid droplets (L). Intercellular canaliculi (red arrow) between two adjacent cells are seen. X4000

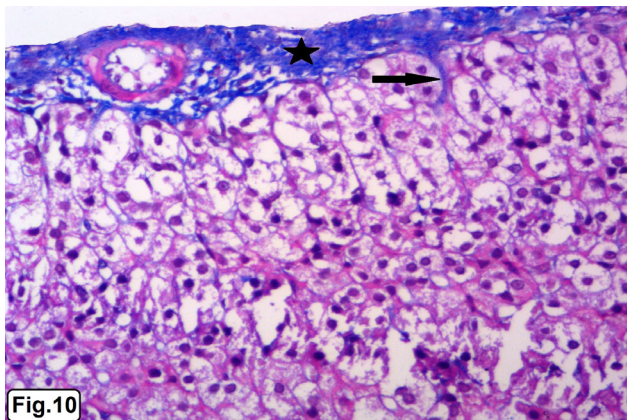


Fig. 10: A section of the adrenal cortex of group III (I/R group) illustrating apparent increased collagen fibers (star) of the capsule and in the extending trabeculae (black arrow) between the arches of zona glomerulosa cells. M.T X200

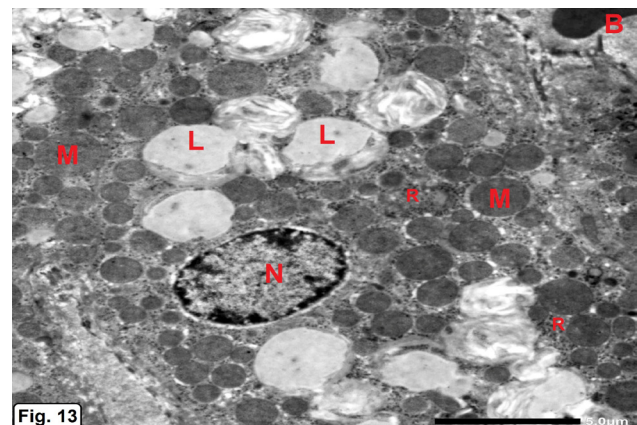


Fig. 13: An electron micrograph of the zona fasciculata cell of group I (SO) illustrating rounded euchromatic nucleus (N), numerous spherical mitochondria of variable sizes (M), free ribosomes (R) and abundant lipid droplets (L). Notice, part of blood sinusoid (B). X1500

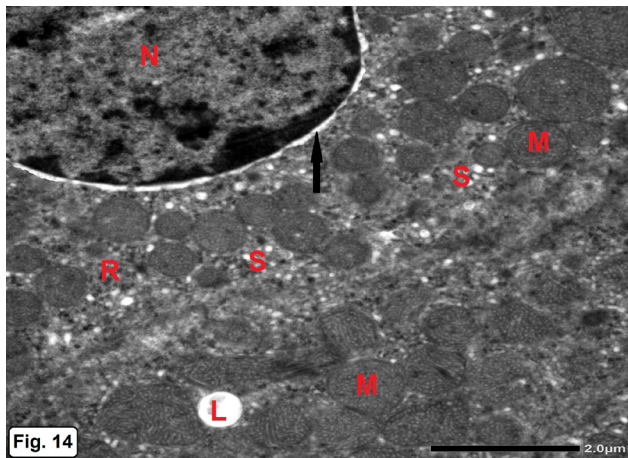


Fig. 14: An electron micrograph of the zona reticularis cell of group I (SO) illustrating part of euchromatic nucleus (N) with perinuclear space (arrow). The cytoplasm contains numerous spherical mitochondria (M) with densely packed vesicular cristae, plenty of smooth endoplasmic reticulum (S), free ribosomes (R) and lipid droplet (L). X4000

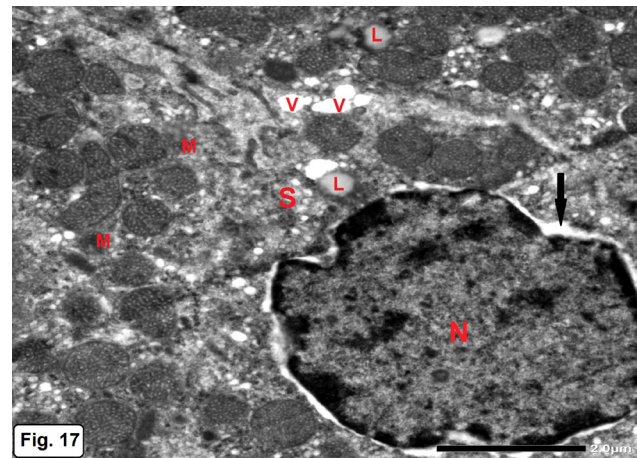


Fig. 17: An electron micrograph of the zona reticularis cell of group III (I/R) illustrating nucleus (N) with irregular nuclear membrane and widened perinuclear space (black arrow). The cytoplasm contains cytoplasmic vacuoles (v), smooth endoplasmic reticulum (S), degenerated mitochondria (M) and lipid droplets (L). X4000

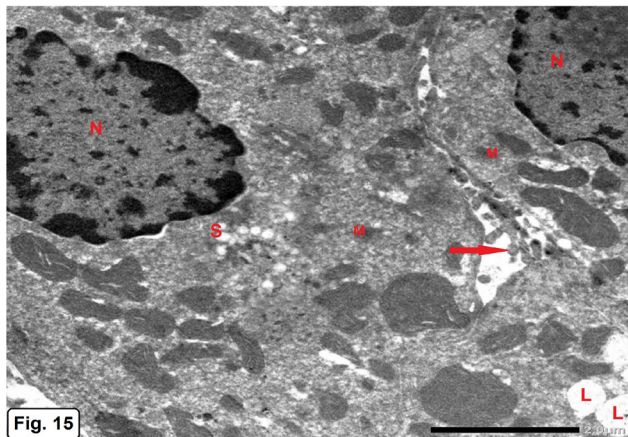


Fig. 15: An electron micrograph of the zona glomerulosa cells of group III (I/R) illustrating nuclei (N) with irregular nuclear membrane, degenerated mitochondria (M), dilated smooth endoplasmic reticulum (S) and some lipid droplets (L). Disrupted intercellular canaliculi (red arrow) between adjacent cells are seen. X4000

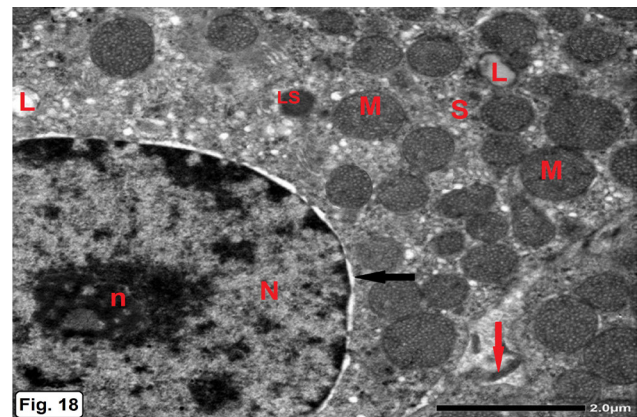


Fig. 18: An electron micrograph of the zona glomerulosa cell of group IV (I/R and L-Arg) illustrating euchromatic nucleus (N) with prominent nucleolus (n) and perinuclear space (black arrow). The cell has vesicular mitochondria (M), smooth endoplasmic reticulum (S), lipid droplets (L) and lysosome (LS). Intercellular canaliculi (red arrow) are seen between two adjacent cells. X4000

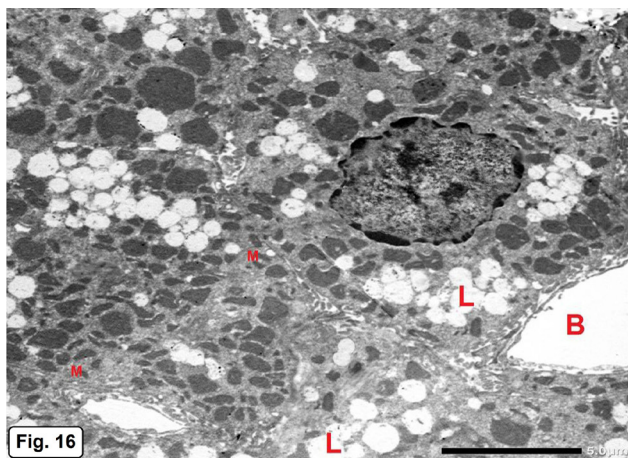


Fig. 16: An electron micrograph of the zona fasciculata cells of group III (I/R) illustrating nucleus (N) with irregular nuclear membrane, degenerated mitochondria (M) and multiple lipid droplets without discernible outline (L). Notice, blood sinusoids (B) between the cells. X1500

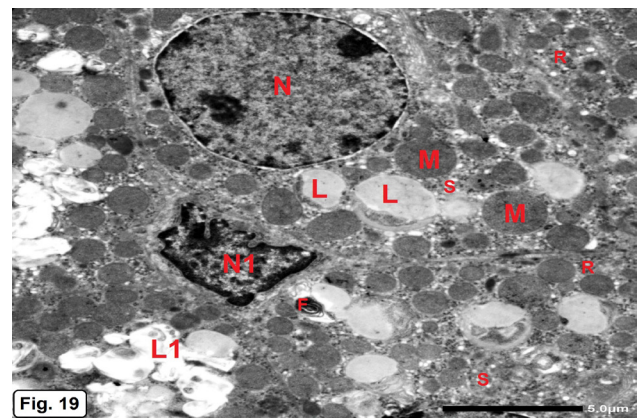


Fig. 19: An electron micrograph of the zona fasciculata cells of group IV (I/R and L-Arg) illustrating rounded euchromatic nucleus (N) with regular nuclear envelope. One cell with shrunken heterochromatic nucleus (N1) is present. Lipid droplets (L), numerous mitochondria (M), smooth endoplasmic reticulum (S), free ribosomes (R) and myelin figure (F) are also observed. Notice, presence of some confluent lipid droplets (L1). X1500

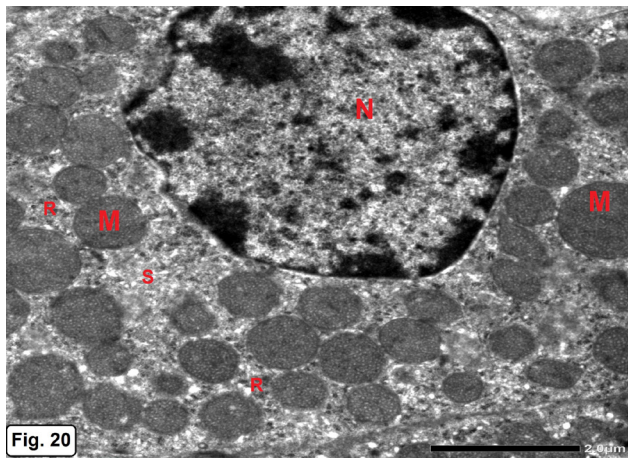


Fig. 20: An electron micrograph of the zona reticularis cell of group IV (I/R and L-Arg) illustrating slightly irregular euchromatic nucleus (N). The cytoplasm contains spherical mitochondria (M) of variable sizes with closely packed vesicular cristae, smooth endoplasmic reticulum (S) and free ribosomes (R). X4000

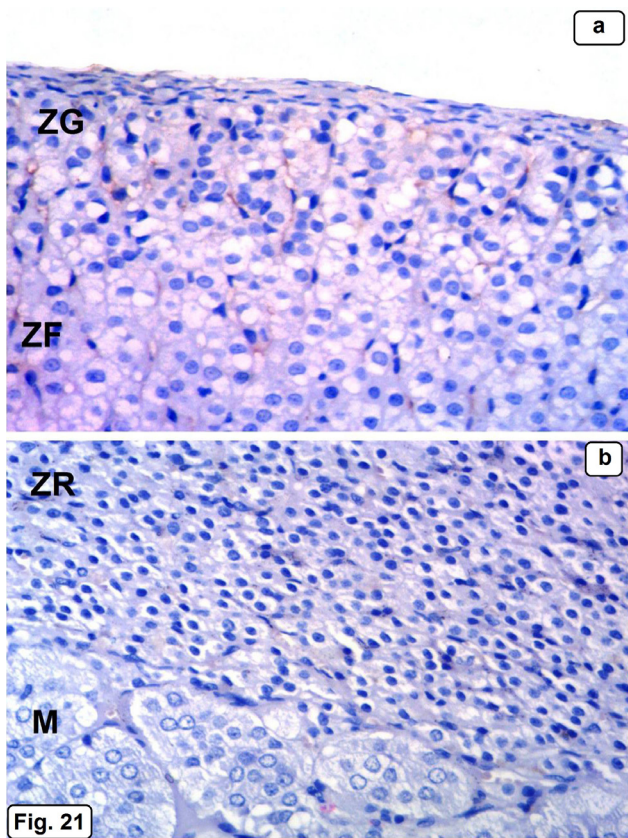


Fig. 21: A section of the adrenal cortex of group I (SO) illustrating (a) negative cytoplasmic immunoreaction for TNF- α in the cells of zona glomerulosa (ZG), zona fasciculata (ZF) and (b) zona reticularis (ZR). TNF- α X200

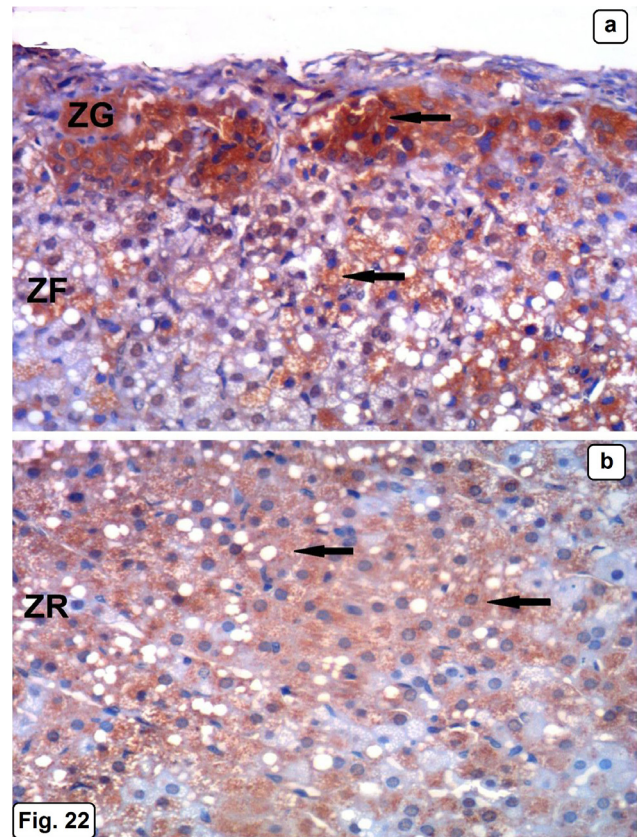


Fig. 22: A photomicrograph of the adrenal cortex of group III (I/R) illustrating (a) strong cytoplasmic immunoreaction for TNF- α in the cells of zona glomerulosa, zona fasciculata and (b) zona reticularis (arrows). TNF- α X200

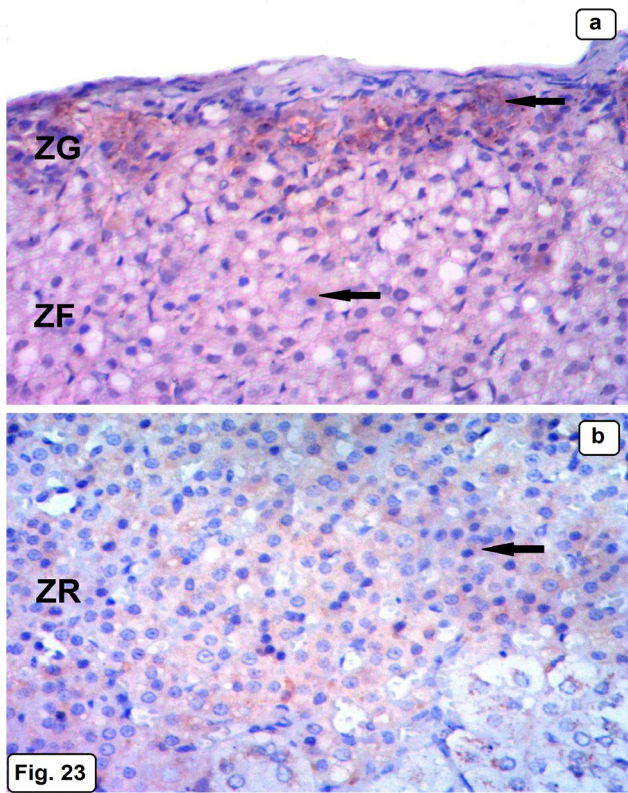


Fig. 23: A section of the adrenal cortex of group IV (I/R and L-Arg) illustrating moderate cytoplasmic immunorexpression for TNF- α in the cells of zona glomerulosa (ZG) and mild expression in zona fasciculata (ZF) and zona reticularis (ZR) (arrows). TNF- α X200

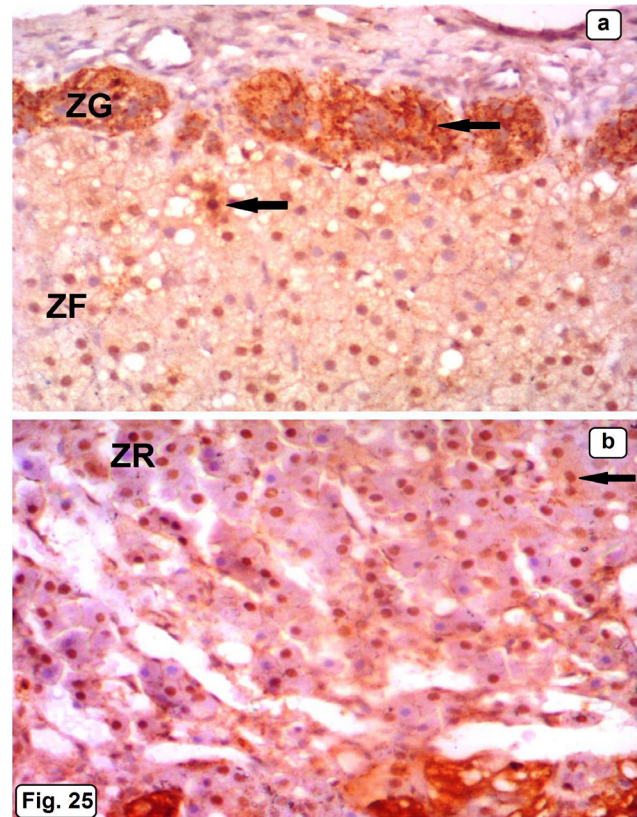


Fig. 25: A section of the adrenal cortex of group III (I/R) illustrating strong positive nuclear and cytoplasmic immunorexpression for caspase 3 in the cells of zona glomerulosa (ZG), zona fasciculata (ZF) and (b) zona reticularis (ZR) (arrows). Caspase-3 X200

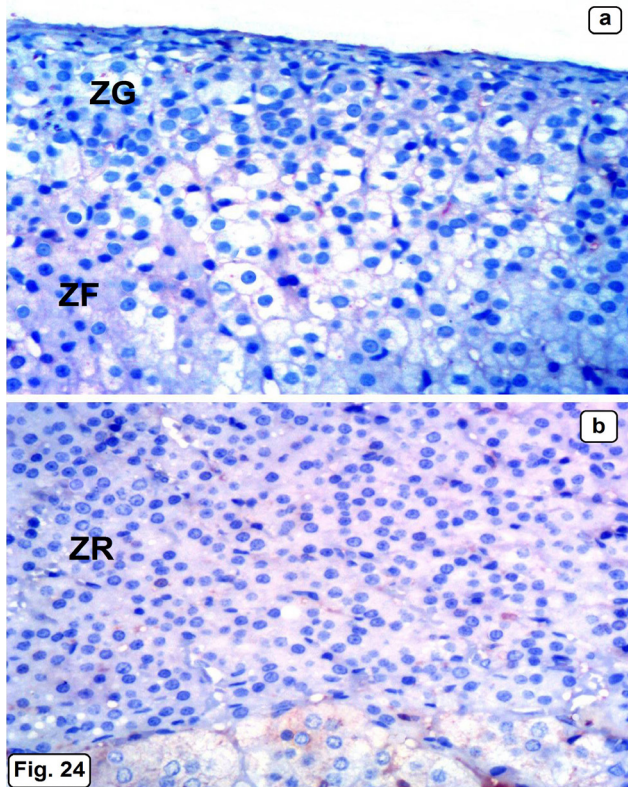


Fig. 24: A section of the adrenal cortex of group I (SO) illustrating negative immunorexpression for caspase 3 in the cells of zona glomerulosa (ZG), zona fasciculata (ZF) and (b) zona reticularis (ZR). Caspase-3 X200

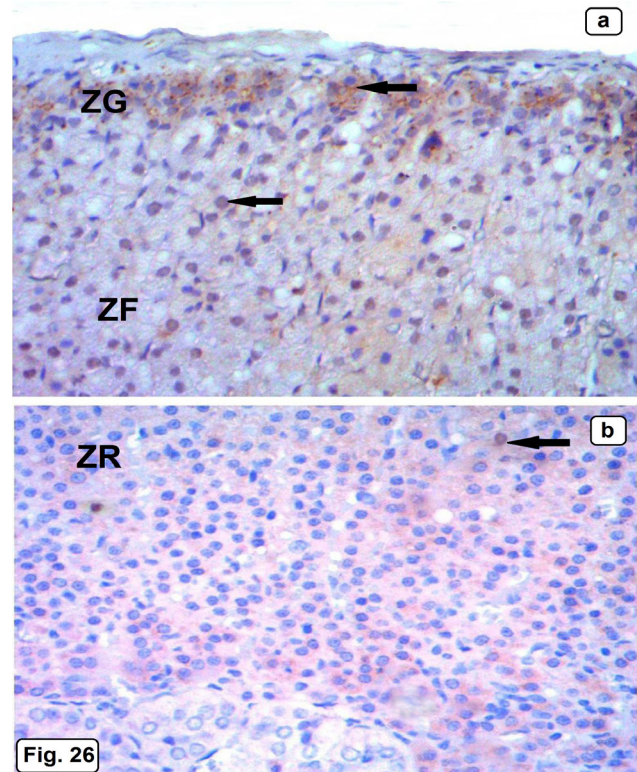


Fig. 26: A section of the adrenal cortex of group IV (I/R and L-Arg) illustrating moderate nuclear and cytoplasmic immunorexpression for caspase 3 in the cells of zona glomerulosa (ZG), zona fasciculata (ZF) and (b) zona reticularis (ZR) (arrows). Caspase-3 X200

Table 1: Mean values ± S.D of AST, ALT and HDL

	I	II	III	IV	
AST (U/L)	83±2.1	82.8±2.1	394±5.1	84.4±2.5	P1=.875 P2=.000 P3=.164 P4=.000
ALT (U/L)	45.4±2	45.9±2.8	296.9±4.9	47.7±3	P1=.656 P2=.000 P3=.067 P4=.000
HDL (mg/dl)	46.1±1.3	46.3±1.3	29.9±2.3	45.8±0.6	P1=.750 P2=.000 P3=.476 P4=.000

Table 2: Mean values ± S.D of MDA and CAT

	I	II	III	IV	
MDA (nmol/ml)	12.6±1	21.5±2	13.3±1.5	13.8±1.6	P1=.475 P2=.000 P3=.071 P4=.000
CAT (u/ml)	500±7.9	467.4±8.1	503.8±5.7	506.3±603	P1=.901 P2=.000 P3=.066 P4=.000

Table 3: Mean values ± S.D of corticosterone and aldosterone

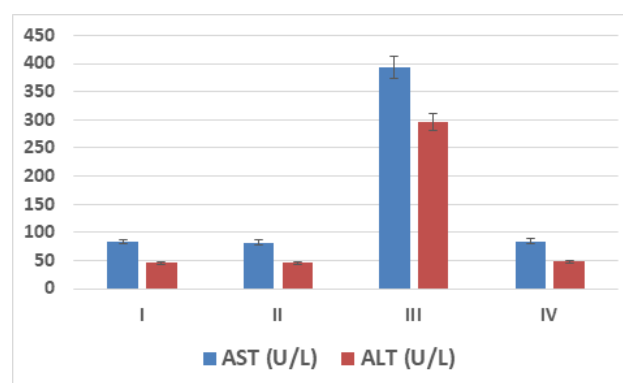
	I	II	III	IV	
Corticosterone (µg/dl)	7.6±0.5	5.7±2.1	7.7±0.4	7.9±0.4	P1=.330 P2=.003 P3=.087 P4=.011
Aldosterone (µg/dl)	6.5±0.5	4.4±2.2	6.7±0.4	6.8±0.3	P1=.353 P2=.004 P3=.093 P4=.010

Table 4: Mean values ± S.D of the thickness of capsule and adrenal cortex

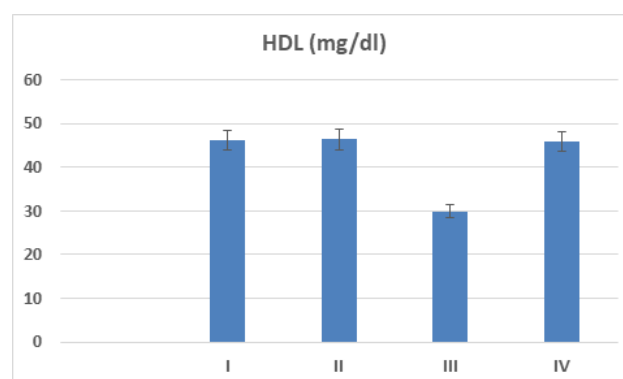
	I	II	III	IV	
Capsule (µm)	12.4±1.6	18.5±2	10.7±1.1	10.6±1.1	P1=.271 P2=.000 P3=.010 P4=.000
Thickness of adrenal cortex (µm)	464.3±4.5	440.5±6.9	466.9±4	468.7±5.3	P1=.398 P2=.000 P3=.060 P4=.000

Table 5: Mean area percentage ± S.D of TNF- α and caspase-3 immune-expression

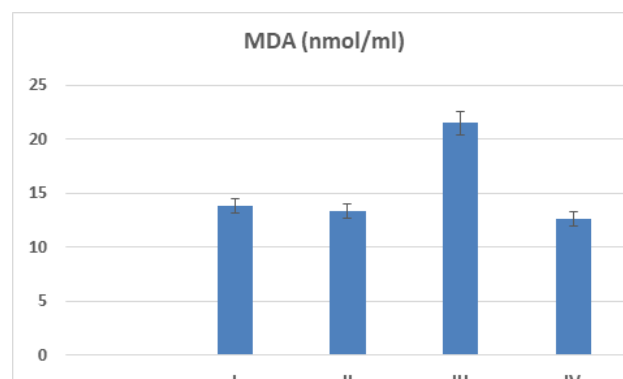
	I	II	III	IV	
TNF-α %	2.2±1.7	10.3±1.1	.2±.0	.1±.1	P1=.114 P2=.000 P3=.002 P4=.000
Caspase-3 %	4.4±3.1	13.1±2.7	0.8±0.3	0.9±0.4	P1=.562 P2=.000 P3=.002 P4=.000



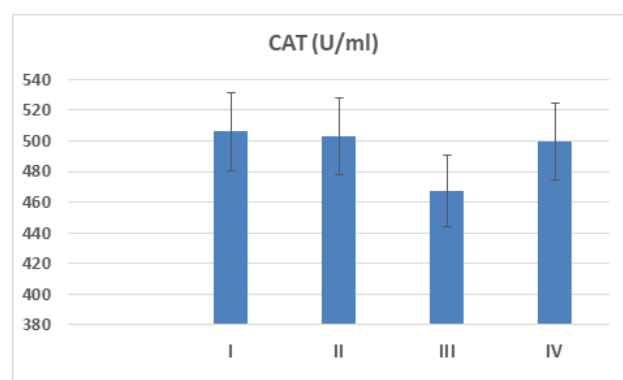
Histogram 1: Mean values of AST and ALT in experimental groups



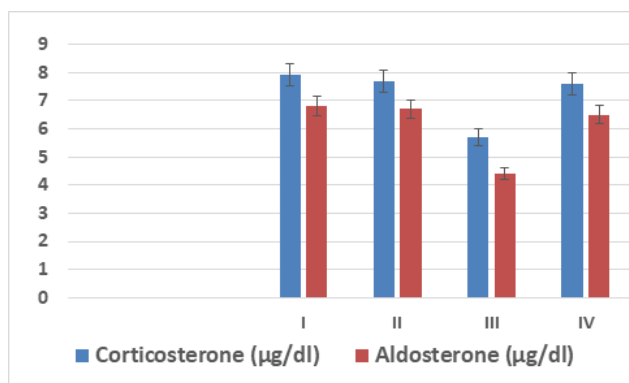
Histogram 2: Mean value of HDL in experimental groups



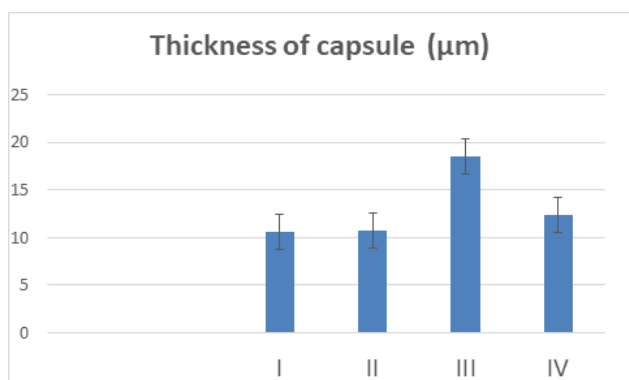
Histogram 3: Mean values of MDA in experimental groups



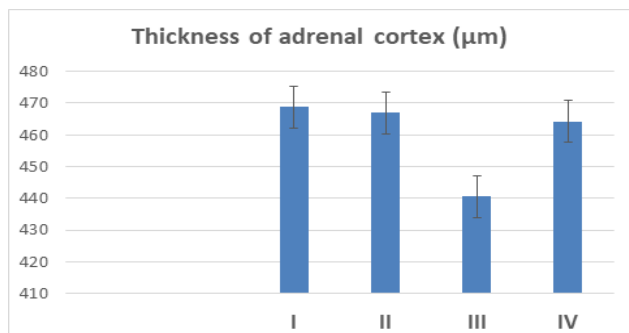
Histogram 4: Mean values of CAT in different experimental groups



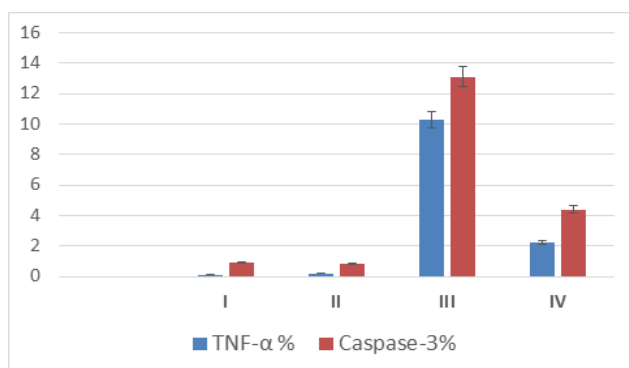
Histogram 5: corticosterone & aldosterone in experimental groups



Histogram 6: Mean values of the thickness of capsule in experimental groups



Histogram 7: Mean values of thickness of adrenal cortex in experimental groups



Histogram 8: Mean TNF-α and caspase-3 immunoreactions in experimental groups

DISCUSSION

Hepatic ischemia and reperfusion become a very important topic during the last years. It is involved in a variety of clinical situations, including hemorrhagic shock, trauma, liver resections, and liver transplantation^[7]. It is one of the primary factors that contribute to postoperative morbidity and death^[25]. Hepatic IRI has a wide range of effects on distant organs such as the kidneys, intestines, pancreas, lungs, and adrenal glands, resulting in MODS^[1]. Hepatic ischemia-reperfusion causes adrenal impairment, which has not been well explored to far. The goal of our research is to determine the impact of hepatic IRI on the function and morphology of adrenal glands. The present work demonstrated that liver IRI led to sever deterioration in liver function as evidenced by a significant increase in plasma levels of ALT and AST compared to control. In hepatic IR injury, emerging reactive oxygen radicals stimulate certain mediators, causing tissue damage and release of AST and ALT enzymes^[26]. Although during ischemia, cell death ensues, paradoxically, tissue reperfusion gives rise to a substantially more severe damage in ischemic tissue and more increase in AST and ALT activities^[2].

The current study demonstrated a significant decrease in serum HDL, Cortisone and Aldosterone levels. This was in accordance with Iwasaki *et al*^[8] who reported relative adrenal insufficiency undergoing liver transplantation. A possible proposed mechanism is HDL reduction after liver transplantation and consequent reduced cortisol formation. According to one study, HDL levels can indicate post-transplant adrenal insufficiency^[27]. At liver ischemia/reperfusion, increased levels of endotoxin and TNF-α have been reported to inhibit steroidogenesis. TNF-α has been shown to inhibit directly steroidogenesis and increase the resistance to cortisol^[7]. Decreased levels of cortical hormones may be also due to affection of mitochondria and endoplasmic reticulum as their biosynthesis occurs inside them by a series of enzymatic reactions^[28]. There was a marked increase in MDA level. Hepatic IRI is a strong oxidant since it produces free radicals which affect the cell membrane and subsequent oxidative damage and cell death. The released free radicals induced an increase in serum lipid peroxidation and MDA level^[29]. In addition, some researchers considered lipid peroxidation is a key factor in IR injury^[2]. In contrast, catalase level was significantly down regulated in this study. This was in agreement with Seifi *et al*^[30] who shown that, ROS are normally eradicated by intrinsic antioxidant enzymes such as catalase enzyme.

In our study, structural examination of sham operation and L- arginine groups revealed normal morphology of the adrenal cortex. However, histological investigation of IR group showed distorted architecture of zona glomerulosa, ballooning of cells of zona fasciculata, vacuolated cytoplasm, numerous pyknotic nuclei, degenerated mitochondria, dilated smooth endoplasmic reticulum, multiple lipid droplets with decreased total thickness of the cortex. This may be explained by that

adrenal cortical cell contain large stores of lipids, the substrate of steroidogenesis. Impaired steroidogenesis led to more steroid precursors accumulation and cytoplasmic vacuolations^[31]. Previously, Osman,^[32] stated that lipid droplets accumulation in the cells of ZF and ZR may be due to impairment in synthesis of glucocorticoids and suppression of steroidogenesis. Multiple lipid droplets occur due to disruption of cytochrome P450 enzymes resulted from increased circulating ROS during liver IR injury that led to inhibition of cholesterol biosynthesis and accumulation of lipid droplets^[33]. Ballooning and hypertrophy of cells of ZF might be a consequence of accumulations of cholesterol / intermediate steroids inside the cells. It was reported that the functional significance of this diffuse cellular hypertrophy might result from increased storage or failure to release steroid precursors^[34]. There were loss of normal cellular arrangement and presence of pyknotic nuclei. These findings were in accordance with Abd El-Gawad *et al*^[35] who found condensed chromatin and abundant lipid droplets together with degenerated mitochondria within cells of ZG and ZF after exposure to hepatic IR.

Presence of degenerated mitochondria with dilated smooth endoplasmic reticulum were noticed in this current study, possibly due to suppression of conversion of cholesterol to steroid hormones and subsequent cholesterol accumulation within these organelles^[36]. These observed ultrastructural changes inhibit steroid synthesis with more accumulation of cholesterol within the mitochondria and so on^[33].

Regarding to Mallory's trichrome stain, excessive deposition of collagen fibers in the capsule and trabeculae was observed in IR group. This was explained by Atiq *et al*^[37] who reported that reactive oxygen species might cause mitochondrial dysfunction that can lead to necrosis, fibrosis and collagen deposition. Moreover, Kamal^[38] demonstrated that injury of cells and their basement membranes lead to an inflammation and immune cells migration to the injury site and the release of cytokines with the overproduction of collagen fibers and fibrosis.

In this work, there was intense increase in caspase-3 immune expression in adrenal cortex of animals of IRI group. Ischemic injury initially led to hypoxia and hyponutrition, so the metabolic cellular products are retained, causing metabolic acidosis. Local inflammation and ROS generation rise when reperfusion is restored, leading in subsequent damage. Autophagy, apoptosis, necrosis, and cell malfunction are all possible outcomes of chronic ischemia-reperfusion injury^[39]. The apoptotic changes observed, was proved by other investigators, they referred that injury of cells in the form of apoptosis occurred after reperfusion. Some apoptotic promoting substances that were released in great amount during IR, trigger apoptosis and cell death^[40]. Apoptosis could be caused via oxidative stress, which is defined as a rise in oxidizing species production or a decline in antioxidant references^[41].

Significant increase in TNF- α immune reaction was detected in IR group. Concomitant with our finding, Jiang *et al*^[42] recorded elevated levels of TNF- α , in the intestinal mucosa after hepatectomy performed under hepatic ischemia and reperfusion. Previous studies showed that release of TNF- α from the reperfused Kupffer cells and a number of proinflammatory molecules released from the reperfused liver, such as cytokine-induced neutrophils-chemo-attractant protein, IL-6, and IL-18, mediate inflammatory response in adrenal gland after hepatic ischemia/reperfusion^[43]. The excessive systemic inflammatory response is clearly defined as a key mechanism of multiple remote organs damage during hepatic ischemia reperfusion where increased circulating levels of transcription factors and proinflammatory cytokines promote the inflammatory changes in the adrenal gland^[44].

The present work reported that administration of L-Arginine to animals of group IV, resulted in improvement of these morphological alterations. The reported ameliorating effect of L-Arginine in the present study may be attributed to increasing of total antioxidant capacity as well as decreasing ALT and AST levels (the hepatic injury markers) and oxidative stress through malonaldehyde decreasing^[45]. Another reason for the beneficial effect of L-Arginine in IR injury could be due to its indirect antioxidant effect through production of NO which has antioxidant and anti-inflammatory activity and inactivates superoxide and reduce lipid peroxidation^[12]. Moreover, Diesen & Kuo^[46] demonstrated that in ethanol-induced hepatic injury, nitric oxide (NO) enhanced microcirculation and reduced hepatic damage, demonstrating that NO has a protective impact in hepatic injury, as its supplementation in liver IRI reduces the extent of IRI and protects remote tissues and organs from its dangerous effect. L-Arg also enhanced mitochondrial structure in cardiac cells during ischemia reperfusion by lowering the level of OFR (oxygen free radical), decreased ischemia-reperfusion injury by inhibiting lipid peroxidation, and reduced apoptosis by modulating the balance between bax mRNA and bcl-2mRNA^[14]. Additionally, growing studies reported that L-arginine stimulates the synthesis of NO and protects the liver from cholestatic damage, evidenced by decreased levels of liver enzymes and lipid peroxidation^[47].

CONCLUSION

From the foregoing data, it could be concluded that hepatic ischemia reperfusion injury (IRI) induced severe adrenal cortical structural changes. These deleterious effects mainly resulted from the systemic oxidative stress state and the released proinflammatory mediators. L-Arginine (L-Arg) has an ameliorative effect that may be mediated through the NO signalling, which increases the activity of antioxidant enzymes, which then scavenge free radicals, or arginine's antioxidant properties. Further researches are necessary to clarify the protective role of L-Arg on adrenal cortex injury occurred in hepatic IRI. The protective effect of L-Arg on the adrenal cortex will help to support its clinical use in the future.

CONFLICT OF INTERESTS

There are no conflicts of interest.

REFERENCES

- Rampes S, Ma D (2019): Hepatic ischemia-reperfusion injury in liver transplant setting: mechanisms and protective strategies, *The Journal of Biomedical Research*, 33(4): 221–234.
- Atalay S, Soylu B, Aykaç A, Velioglu A *et al* (2019): Protective effects of spironolactone against hepatic ischemia/reperfusion injury in rats, *Turk J Surg*; 35 (4): 285-292.
- Cannistr M, Ruggiero M, Zullo A *et al* (2016): Hepatic ischemia reperfusion injury: A systematic review of literature and the role of current drugs and biomarkers, *International Journal of Surgery*; 33 557-570.
- Kim H J, Joe Y, Yu J K, Chen Y *et al* (2015): Carbon monoxide protects against hepatic ischemia/reperfusion injury by modulating the miR 34a/SIRT1 pathway. *Biochimica et Biophysica Acta (BBA) Molecular Basis of Disease* 1852 , 1550–1559.
- Orellana C, Villagrán R, Zang J, Rodrigo R (2019): The role of oxidative stress in hepatic ischemia reperfusion injury: potential target for interventions in liver transplantation, *Clin Res Trials*, Volume 5: 1-4.
- Harvey P W (2015). *Endocrine disruption of adrenocortical function, Endocrine disruption and human health* (219–235). Philip W. Harvey, UK: Elsevier Inc.
- Nastos C, Kalimeris K, Papoutsidakis N, Tasoulis M K, Lykoudis P *et al* (2014): Global consequences of liver ischemia/reperfusion injury. *Oxidative Medicine and Cellular Longevity*, 2014, 1–13.
- Iwasaki T, Tominaga M, Fukumoto T, Kusunoki N, Sugimoto T (2006): Relative adrenal insufficiency manifested with multiple organ dysfunction in a liver transplant patient. *Liver Transplantation*, 12, 1896–1899.
- Wu G, Bazer FW, Davis TA, Jaeger LA, Johnson GA, Kim SW (2007):. Important roles for the arginine family of amino acids in swine nutrition and production. *Livest Sci* 2007; 112: 8–22.
- Hou Y, Wu G (2017) Nutritionally nonessential amino acids: a misnomer in nutritional sciences. *Adv Nutr* 8:137–139. doi:10.3945/ an.116.012971
- Quan L, Yulan L, Zhengquan C, Huiling Z (2012): Dietary L-arginine supplementation alleviates liver injury caused by *Escherichia coli* LPS in weaned pigs *Innate Immunity*; 18(6) 804–814.
- Hamad S R, Mohamed H R (2020): Modulation of Monosodium Glutamate Induced Histological Injuries, *Histomorphometrical Alterations and DNA Damage in the Mice Hepatic and Renal Tissues by Oral Administration Nano-Cerium Oxide and L-arginine and their Combination*, *EJH*; 43(4): 1034-1046.
- Al-Dalaen S, Alzyouo J, Al-Qtaitat A (2016): The Effects of L-Arginine in Modulating Liver Antioxidant Biomarkers within Carbon Tetrachloride Induced Hepatotoxicity: Experimental Study in Rats; *Biomedical & Pharmacology Journal* Vol. 9(1), 293-298 .
- Chen D, Huang L, Jinbo H, Song D, Yingchun M, Wang W (2014): Effect of L-arginine on Function of Mitochondria in Ischemia –Reperfusion Myocardial Cell in Rabbits Chen *et al.*, *J Cell Sci Ther*, 5:3 DOI: 10.4172/2157-7013.1000166
- Pereda J, Gómez-Cambronero L, Alberola A, Fabregat G *et al* (2006): "Co-administration of pentoxifylline and thiopental causes death by acute pulmonary oedema in rats". *British Journal of Pharmacology*. 149 (4):450–5.
- Kamel M Y, Aziz N, El Tahawy N F G (2015). Different effects of glucocorticoids; dexamethasone and NSAIDS; indomethacin on hepatic and renal injury following normothermic hepatic ischemia reperfusion. *Journal of International Research in Medical and Pharmaceutical Sciences*, 2(1), 1–15.
- Bergmeyer H U, Grabl M H E Walter H E (1983): *Methods of Enzymatic Analysis*, Verlag Chemie, Weinheim, Germany .
- Hinchliffe E, Carter S, Owen LJ, Keevil BG (2013): Quantitation of aldosterone in human plasma by ultra high performance liquid chromatography tandem mass spectrometry. *J Chromatogr B Anal Technol Biomed Life Sci*; 913-914:19-23
- Al Bazii W (2014): Estimation of some oxidative stress parameters in the serum and cerebellum of ovariectomized rats. *Journal of Kerbala University*, 12, 87–94.
- Ahmed H H, Abdalla M S, Eskander E F, Al Khadragy M F (2012): Hypolipidemic influence of *Sargassum subrepandum*: Mechanism of action. *European Review for Medical and Pharmacological Sciences*, 16, 112–120.
- Suvarna K, Layton C, Bancroft J (2013): *Theory and Practice of Histological Techniques*, seventh ed. Churchill Livingstone of Elsevier, Philadelphia, USA, pp.173–214.
- Graham L, Orenstein J M (2007): Processing tissue and cells for transmission electron microscopy in diagnostic pathology and research. *Nature Protocols*, 2, 2439–2450
- Sabry MM, Elkalawy SAE, Abo-Elnour RKD (2014): Histological and immunohistochemical study on the effect of stem cell therapy on bleomycin induced pulmonary fibrosis in albino rat. *Int J Stem Cells*. 7(1): 33–42.

24. Emsley R, Dunn G, White I (2010): Mediation and moderation of treatment effects in randomized controlled trials of complex interventions. *Stat Methods MedRes*; 19:237–270.
25. Mendes-Braz M, Elias-Miro M, Jimenez-Castro M.B, Casillas-Ramirez A, Ramalho F.S, Peralta C (2012): “The current state of knowledge of hepatic ischemia-reperfusion injury based on its study in experimental models,” *Journal of Biomedicine and Biotechnology*, vol. 2012, Article ID 298657, 20 pages,.
26. Kadkhodae M, Mikaeili S, Zahmatkesh M, Golab F, Seifi B, Arab, H, Mahdavi Mazdeh M (2012): Alteration of renal functional, oxidative stress and inflammatory indices following hepatic ischemia-reperfusion. *General Physiology and Biophysics*, 31, 195–202.
27. Marik P E, Gayowski T, Starzl T.E (2005): “The hepatoadrenal syndrome: a common yet unrecognized clinical condition,” *Critical Care Medicine*, vol. 33, no. 6, pp. 1254–1259.
28. Inomata A, Sasano H (2015): Practical approaches for evaluating adrenal toxicity in nonclinical safety assessment. *J Toxicol Pathol* ;28(3):125-32.
29. Razali N, Mat Junit S, Ariffin A, Ramli N S F & Abdul Aziz A (2015): Polyphenols from the extract and fraction of *T. indica* seeds protected HepG2 cells against oxidative stress. *BMC Complementary and Alternative Medicine*, 15, 438.
30. Seifi B, Kadkhodae M, Delavari F, Mikaeili S, Shams S & Ostad S N (2012): Pretreatment with pentoxifylline and N acetylcysteine in liver ischemia reperfusion induced renal injury and Renal Failure 34, 610–615.
31. Evans, G.O. (2009). *Animal clinical chemistry: A practical handbook for toxicologists and biomedical researchers*. CRC Press.
32. Osman H (2010): Morphological evaluation on the protective effect of curcumin on nicotine induced histological changes of the adrenal cortex in mice. *Egyptian Journal of Histology*, 33, 552–559.
33. El Tahawy N F G, Abozaid S M M (2019): The possible structural changes in the adrenal gland cortex after induction of hepatic ischemia reperfusion – injury in male albino rats: Light and electron microscopic study *J Cell Physiol*. 2019;234:15487-15495.
34. Harvey PW, Sutcliffe (2010): Adrenocortical hypertrophy: Establishing cause and toxicological significance. *J Appl Toxicol*;30: 617-26.
35. Abd El-Gawad FA, Zaki SM, El-Shaarawy EA, Radwan RA, Aboul-Hoda BE (2016): Histological and histomorphometric reorganization of the adrenal cortex of adolescent male albino rat following exposure to stress. *Med J Cairo Univ*; 84 (1): 1107 - 1112.
36. Elshennawy W W, Aboelwafa H R (2011): Structural and ultrastructural alterations in mammalian adrenal cortex under influence of steroidogenesis inhibitor drug. *Journal of American Science*, 7.567–576.
37. Atiq M, Davia J C, Lamps L W, Beland S S, Rose J E (2009): Amiodarone induced liver cirrhosis. Report of two cases. *Journal of Gastrointestinal and Liver Diseases* 18: 233-235.
38. Kamal H M (2014): The possible protective effect of exercise on liver damage following hind-limb ischemia-reperfusion injury in the adult male albino rat: light and electron microscopic study. *The Egyptian Journal of Histology* 37(1): 146-158.
39. Ling Q, Yu X, Wang T, Wang SG, Ye ZQ, Liu JH (2017): Roles of the Exogenous H₂S-Mediated SR-A Signaling Pathway in Renal Ischemia/ Reperfusion Injury in Regulating Endoplasmic Reticulum Stress-Induced Autophagy in a Rat Model. *Cell Physiol Biochem*;41:2461-2474.
40. Meng-Yu W, Giou-Teng Y, Wan-Ting L, Andy Po-Yi T (2018): Current Mechanistic Concepts in Ischemia and Reperfusion Injury *Cell Physiol Biochem*;46:1650-1667 DOI: 10.1159/00048924
41. Rasha I A, Reneah R B, Hala Z E M (2018): The protective role of the exercise on the remote lung damage following ischemia/reperfusion injury in the hind-limb of the adult male albino rat: A histological and a morphometric study *The Egyptian Journal of Anatomy*, Jan. 2018; 41(1):10-19.
42. Jiang H, F.Meng FW, Li J, Tong H, Qiao X (2007): “Splenectomy ameliorates acute multiple organ damage induced by liver warm ischemia reperfusion in rats,” *Surgery*, vol. 141, no. 1, pp. 32–40,.
43. Marik P E, Gayowski T, Starzl T E (2005): “The hepatoadrenal syndrome: a common yet unrecognized clinical condition,” *Critical Care Medicine*, vol. 33, no. 6, pp. 1254–1259,.
44. Levy R M, Mollen K P, Prince J M (2007): “Systemic inflammation and remote organ injury following trauma require HMGB1,” *American Journal of Physiology—Regulatory Integrative and Comparative Physiology*, vol. 293, no. 4, pp. R1538–R1544,.
45. Abo Zeid, El Saka MH, Shafik NM. (2012): Effect of combination of L-arginine and N-acetyl cysteine in rat model of renal ischemia-reperfusion injury. *J Am Sci.*; 8(10): 814– 921, doi: 10.7537/j.issn.1545-1003.
46. Diesen DL , Kuo PC (2010): Nitric oxide and redox regulation in the liver: Part I. General considerations and redox biology in hepatitis. *J Surg Res*. 162(1):95-109
47. Ozsoy Y, Ozsoy M, Coskun T, Naml K *et al* (2011): The Effects of L-Arginine on Liver Damage in Experimental Acute Cholestasis an Immunohistochemical Study *HPB Surgery Volume 2011*, Article ID 306069, 5 pages doi:10.1155/2011/306069

الملخص العربي

تأثير وقف تدفق الدم الكبدى واعادة الارواء على قشرة الغدة الكظرية لذكور الجرذان البيضاء البالغة والدور الوقائي المحتمل ل ارجينين: دراسة كيميائية حيوية وهستولوجية وهستوكيميائية مناعية

اميرة فهمي علي ونادية سعيد بدوي خير

قسم الأنسجة - كلية الطب؛ جامعة المنوفية، مصر

مقدمة البحث: تحدث إصابة وقف تدفق الدم الكبدى واعادة الارواء بشكل كبير أثناء زراعة الكبد. مما يؤثر بشكل خطير على وظائف الكبد ، وأنه مسؤول عن ١٥ ٪ من فشل الأعضاء المبكر وفي بعض الحالات يمكن أن يؤدي إلى متلازمة خلل وظيفي متعدد الأعضاء التي لها معدلات عالية من الوفيات . وقد وجد ان ل ارجينين يخفف من اثار وقف تدفق الدم الكبدى واعادة الارواء من خلال آليات مختلفة

الهدف من البحث : هو تقييم تأثير وقف تدفق الدم الكبدى واعادة الارواء على قشرة الغدة الكظرية لذكور الجرذان البيضاء البالغة والتأثير الوقائي المحتمل ل ارجينين

مواد وطرق البحث : تم استخدام اثنا وثلاثين من ذكور الجرذان البيضاء في الدراسة الحالية. تم تقسيم الحيوانات إلى المجموعة الأولى (مجموعة الشام) ، المجموعة الثانية (مجموعة ل ارجينين) ، المجموعة الثالثة (مجموعة وقف تدفق الدم الكبدى واعادة الارواء) والمجموعة الرابعة (مجموعة وقف تدفق الدم الكبدى واعادة الارواء و ل ارجينين). في نهاية الإجراء ، وتم جمع عينات الدم من أجل الدراسة البيوكيميائية وتمت معالجة أنسجة الغدة الكظرية من أجل الدراسات الهستولوجية والهستوكيميائية المناعية.

النتائج: لقد اظهرت النتائج ان خلايا قشرة الغدة الكظرية لمجموعة وقف تدفق الدم الكبدى واعادة الارواء غير منظمه, منتفخه , انويتها ضامره وفي بعض الخلايا متحلله والسيتوبلازم به فجوات .كما لوحظ زيادة ملحوظة في مستويات إنزيمات الكبد في الدم ، وزيادة في مستوى MDA وانخفاض ملحوظ في مستوى CAT مقارنة بمجموعة التحكم. تم تحسين هذه التغييرات بواسطة ل ارجينين.

الخلاصة: ثبت أن وقف تدفق الدم الكبدى واعادة الارواء يسبب تغيرات نسيجية في قشرة الغدة الكظرية والتي يمكن تحسينها عن طريق إعطاء ل ارجينين.